

Enzymatic Probing of Model Lipid Membranes: Phospholipase A2 Activity toward Monolayers Modified by Oxicam NSAIDs

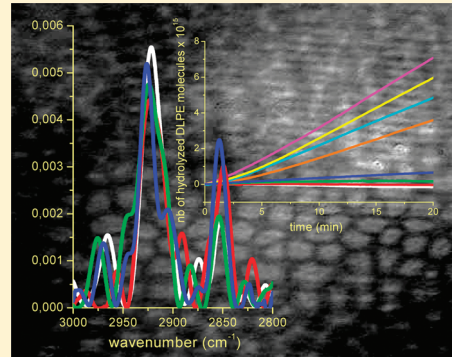
Katarzyna Czapla,^{†,‡} Beata Korchowiec,^{†,‡} Monika Orlof,^{†,‡} Jenifer Rubio Magnieto,^{‡,§} and Ewa Rogalska^{*,†}

[†]Department of Physical Chemistry and Electrochemistry, Faculty of Chemistry, Jagiellonian University, ul. R. Ingardena 3, 30-060 Krakow, Poland

[‡]Structure et Réactivité des Systèmes Moléculaires Complexes, BP 239, CNRS/Nancy Université, 54506 Vandoeuvre-lès-Nancy cedex, France

[§]Departamento de Química Inorgánica y Orgánica, Universitat Jaume I, Avd. Sos Baynat s/n, Castellón, Spain

ABSTRACT: Three nonsteroidal anti-inflammatory oxicam drugs, namely meloxicam, piroxicam, and tenoxicam, were used to modify the properties of monomolecular films formed with 1,2-dilauroyl-*sn*-glycero-3-phosphocholine, 1,2-dilauroyl-*sn*-glycero-3-phosphoethanolamine, or 1,2-dilauroyl-*sn*-glycero-3-phospho-(1-*rac*-glycerol). These systems were examined via surface pressure and surface electrical potential measurements, polarization modulation infrared reflection absorption spectroscopy, and Brewster angle microscopy. Moreover, phospholipase A2 activity was used to differentiate between the three drugs. Our results reveal that the oxicams studied modify membrane properties, namely hydration of the lipid polar heads, orientation of the molecules, and morphology of the domains. Phospholipase A2 was shown to be sensitive to the presence of the drugs in the systems studied; the activity of the enzyme correlates with the effect of meloxicam, piroxicam, and tenoxicam on the monolayer properties. The latter indicates that the anti-inflammatory action of oxicams may be related to interference with phospholipase activity in addition to cyclooxygenase inhibition.



INTRODUCTION

Nonsteroidal anti-inflammatory drugs (NSAIDs) are inhibitors of prostaglandin H synthase, more commonly referred to as cyclooxygenase (COX).¹ To reach this membrane protein, NSAIDs must pass through the cell membrane and, in addition, either enter the interior of the endoplasmic membrane or pass through the plasma membrane.^{2–4} It is increasingly accepted that COX-1/COX-2, cytosolic phospholipase A2 (cPLA2), and prostacyclin synthase are colocalized in the nuclear envelope and endoplasmic reticulum and are functionally coupled to facilitate the transfer of intermediate metabolites.^{5,6} Importantly, phospholipase A2 (PLA2), which liberates arachidonic acid used by COX, is activated upon adsorption to the membrane.⁷

A better understanding of the complex, membrane-related processes of COX inhibition can be obtained from studies using model lipid membranes. It was shown recently that meloxicam, lornoxicam, and nimesulide increase the fluidities of different model membranes in a concentration-dependent manner. It was proposed that the induced changes in lipid dynamics may modulate the activity of inflammatory enzymes.⁸ Indeed, depending on the membrane packing, the conformation of the enzymes, as well as the interactions between the enzymes and the membrane-bound substrates, may be modified.⁹

We showed recently that the effects of different NSAIDs on model lipid membranes are different, in spite of structural similarities of those molecules.¹⁰ Compared to native lipid

membranes in the form of bilayers, lipid monomolecular films (Langmuir films) are readily amenable to study via a rich variety of experimental techniques. Studies of the interaction between some drugs and model monolayer membranes have already been performed.^{11,12} The Langmuir technique was used in the study of the interaction between NSAIDs and human gastric mucosal phospholipids¹³ and with the lipids of the outer and inner leaflets of eukaryotic cells.¹⁴ The Langmuir technique was also used to gain insight into the mechanism of the gastrointestinal disorders provoked by NSAIDs.¹⁵

Our preliminary work demonstrated that meloxicam (MEL) has an impact on the rate of the lipolysis catalyzed by PLA2.¹⁶ Indeed, the enzymatic experiments showed that MEL reduces the PLA2 activity in the presence of 5.0 mM Ca²⁺. This result suggested that the inhibition of PLA2 by NSAIDs could reduce production of arachidonic acid, which is the limiting factor for prostaglandin production, and in this way prevent inflammation regardless of the inhibition of COX-2. Here, to check the generality of the NSAID-related effect, 1,2-dilauroyl-*sn*-glycero-3-phosphocholine (DLPC), 1,2-dilauroyl-*sn*-glycero-3-phosphoethanolamine (DLPE), and 1,2-dilauroyl-*sn*-glycero-3-phospho-(1-*rac*-glycerol) (DLPG) were used as representative lipid

Received: March 23, 2011

Revised: June 13, 2011

Published: June 17, 2011

components of eukaryotic membranes. The saturated lipids were chosen to avoid oxidation of the hydrocarbon chains; medium-length chains were necessary for monitoring enzyme activity.¹⁷ The monomolecular films were formed with DLPC, DLPE, and DLPG on aqueous subphases containing three different NSAIDs, namely tenoxicam (TEN), piroxicam (PIR), or meloxicam. The three oxicams used are structurally closely related molecules resulting from isosteric replacement in drug design.¹⁸

The interactions of TEN, PIR, or MEL with lipid monolayers were monitored via simultaneous measurements of surface pressure (Π) and surface electric potential (ΔV), and by polarization modulation infrared reflection absorption spectroscopy (PM-IRRAS). Moreover, the lateral organization and morphology of the monolayers formed in the presence of TEN, PIR, or MEL were investigated using Brewster angle microscopy (BAM). This physicochemical characterization of the monolayers prepared the ground for the enzymatic lipolysis experiments.

■ EXPERIMENTAL SECTION

Materials and Reagents. 1,2-Dilauroyl-sn-glycero-3-phosphocholine (P1263, ≥99%), 1,2-dilauroyl-sn-glycero-3-phosphoethanolamine (P6270, ≥98%), tenoxicam ((3E)-3-[hydroxy(pyridin-2-ylamino)methylene]-2-methyl-2,3-dihydro-4H-thieno[2,3-e][1,2]thiazin-4-one 1,1-dioxide; T0909, ≥99%), and piroxicam ((8E)-8-[hydroxy(pyridin-2-ylamino)methylidene]-9-methyl-10,10-dioxo-10 λ^6 -thia-9-azabicyclo[4.4.0]deca-1,3,5-trien-7-one; P5654, ≥98%) were from Sigma-Aldrich; meloxicam (4-hydroxy-2-methyl-N-(5-methyl-2-thiazolyl)-2H-1,2-benzothiazine-3-carboxamide-1,1-dioxide; >99%) was from Boehringer Ingelheim; and 1,2-dilauroyl-sn-glycero-3-phospho-(1-rac-glycerol) was from Avanti Polar Lipids (840435P, ≥99%). Aqueous solutions containing TEN, PIR, or MEL had 11 μM (pH 5.6) concentration. This concentration was chosen because it is below the solubility limit of MEL in water; the latter is the least soluble among the three oxicams.^{16,18–20} Appropriate amounts of NSAIDs were dissolved in 1 L of Milli-Q degassed water; the solutions were stirred using a magnetic stirrer for 24 h at 20 °C and then filtered through a 0.45 μm PTFE filter. Chloroform and methanol (both ~99.9% pure) used for preparing phospholipid solutions were from Sigma-Aldrich. Porcine pancreatic phospholipase A2 (SIGMA, P6534; 1020 units mg^{-1} , concentration 2.6 mg mL⁻¹) was used in DLPC, DLPE, and DLPG monolayer lipolysis experiments. Calcium chloride dihydrate ($\text{CaCl}_2 \cdot 2\text{H}_2\text{O}$, purity ≥99%) was from Sigma-Aldrich. Milli-Q water (pH 5.6) used in the experiments contained 4.67 ng mL⁻¹ (0.116 μM) of Ca^{2+} cations, as determined using an inductively coupled plasma mass spectrometer (ICP-MS, ELAN DRC-e, PerkinElmer).

Compression Isotherms and Brewster Angle Microscopy. The surface pressure and electric surface potential measurements were carried out with a KSV 5000 Langmuir balance (KSV Instruments Ltd., Helsinki, Finland). A Teflon trough [58 cm (length) × 15 cm (width) × 1 cm (depth)] with two hydrophilic Delrin barriers (symmetric compression) was used in compression isotherm experiments. The system was equipped with an electrobalance and a platinum Wilhelmy plate (perimeter 3.94 cm) as surface pressure sensor. Surface potential was measured using a KSV Spot 1 with a vibrating plate electrode and a steel counter electrode immersed in the subphase. The apparatus was enclosed in a Plexiglas box, and temperature was kept constant at 20 °C. All solvents used for cleaning the trough

and the barriers were of analytical grade. Aqueous subphases for monolayer experiments were prepared with Milli-Q water, which had a surface tension of 72.8 mN m⁻¹ at 20 °C, pH 5.6. Because oxicams are absorbed from the intestinal region, the latter value of pH was chosen, as it corresponds to duodenum conditions.¹⁸ Monolayers were spread from calibrated solutions (concentration around 0.5 mg mL⁻¹) of DLPC in chloroform and DLPE and DLPG in chloroform/methanol mixture (3:1 v/v) using a microsyringe (Hamilton Co., USA). After an equilibration time of 20 min, the films were compressed at a rate of 5 mm min⁻¹ barrier⁻¹ by two symmetrically moving barriers. A PC and KSV software were used to control the experiments. Each compression isotherm was performed at least three times. The standard deviation was ±0.5 Å² for mean molecular area (A), ±0.2 mN m⁻¹ for surface pressure, and ±0.005 V for surface potential measurements.

The compression isotherms allowed calculating the compressibility modulus (C_s^{-1} ; $C_s^{-1} = -A(\partial\Pi/\partial A)_T$). The collapse parameters ΔV_{coll} , Π_{coll} , and A_{coll} , as well as the parameters corresponding to surface pressures of 15 and 30 mN m⁻¹, were determined directly from the compression isotherms.

The morphologies of the studied films were visualized using a computer-interfaced KSV 2000 Langmuir balance combined with a Brewster angle microscope (KSV Optrel BAM 300, Helsinki, Finland). The Teflon trough dimensions were 58 cm (l) × 6.5 cm (w) × 1 cm (d); other experimental conditions were as described above.

Polarization Modulation Infrared Reflection Absorption Spectroscopy. The PM-IRRAS spectra of phospholipid monolayers spread on pure water or on aqueous solutions of drug molecules were registered at 20 °C. The Teflon trough dimensions were 36.5 cm (l) × 7.5 cm (w) × 0.5 cm (d); other experimental conditions were as described in the preceding paragraph. The PM-IRRAS measurements were performed using a KSV PMI 550 instrument (KSV Instruments Ltd., Helsinki, Finland). The PMI 550 contains a compact Fourier transform IR spectrometer equipped with a polarization-modulation (PM) unit on one arm of a goniometer and an MCT detector on the other arm. The incident angle of the light beam can be freely chosen between 40 and 90°; here, the incident angle was 75°. The spectrometer and the PM unit operate at different frequencies, allowing separation of the two signals at the detector. The PM unit consists of a photoelastic modulator (PEM), which is an IR-transparent, ZnSe piezoelectric lens. The incoming light is continuously modulated between s- and p-polarizations at a frequency of 74 kHz. This allows simultaneous measurement of spectra for the two polarizations, with the difference providing surface-specific information and the sum providing the reference spectrum. As the spectra are measured simultaneously, the effect of water vapor is largely removed. The PM-IRRAS spectra of the film-covered surface, $S(f)$, as well as that of pure water, $S(w)$, were measured, and the normalized difference $\Delta S/S = [S(f) - S(w)]/S(w)$ is reported. Six thousand interferogram scans (10 scans/s) have been acquired for each spectrum. In the mid-IR region, the wavenumber at which the half-wave retardation takes place can be freely selected. Here, the maximum of PEM efficiency was set either to 1500 or to 2900 cm⁻¹ for analyzing the carbonyl stretching or methylene stretching regions of the spectra, respectively. The spectral range of the device is 800–4000 cm⁻¹ and the resolution is 8 cm⁻¹.

Enzymatic Lipolysis. Porcine pancreatic phospholipase A2 was used for catalyzing the lipolysis of monolayers formed with

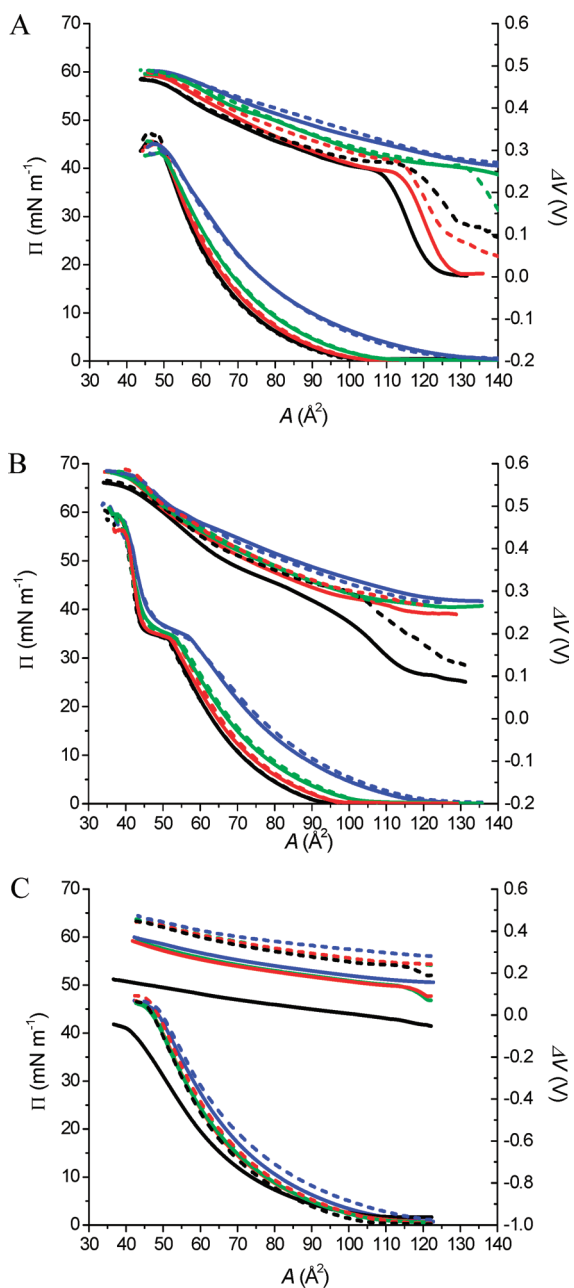


Figure 1. Compression isotherms (Π – A , lower eight curves; ΔV – A , upper eight curves) of DLPC (A), DLPE (B), and DLPG (C) monolayers spread on different subphases. Subphases: NSAID-free water subphase (black); 11 μM TEN (red); 11 μM PIR (green); 11 μM MEL (blue); 0.116 μM Ca^{2+} (solid lines); 5.0 mM CaCl_2 (dotted lines). Temperature 20 °C.

DLPC, DLPE, or DLPG. The lipolysis reactions were performed at constant surface pressures of 15 or 30 mN m^{-1} . The subphases were prepared with Milli-Q water containing 0.116 μM (4.67 $\mu\text{g L}^{-1}$) Ca^{2+} cations (pH 5.6). Depending on the experiment, Milli-Q water contained also CaCl_2 (concentration 5 mM, pH 6.0), TEN, PIR, or MEL (concentration 11 μM , pH 5.6). The experiments were performed with a KSV 3000 Langmuir balance (KSV, Helsinki, Finland) and a zero-order trough¹⁷ with a symmetric compression. A zero-order trough was composed of a reaction compartment [5.5 cm (w) \times 3.0 cm (l) \times 0.5 cm (d)] and two

reservoir compartments [16 cm (l) \times 7.5 cm (w) \times 0.5 cm (d)] communicating by means of two narrow surface channels. The enzyme was injected under the film in the reaction compartment only, whereas the substrate film covered all three compartments. The reservoir compartments contained mobile barriers, which were used to compensate for substrate molecules removed from the film in the reaction compartment by enzyme hydrolysis, thereby keeping surface pressure constant. Surface pressure was measured in the reservoir compartment with a Wilhelmy plate (perimeter 3.94 cm) attached to an electro-microbalance, connected in turn to a computer controlling the movement of the mobile barriers. The subphase was thermostatically maintained at 20 °C and was continuously agitated in the reaction compartment with a 1 cm magnetic stirrer moving at 250 rpm. The enzyme solution was injected through the film with a Hamilton syringe (2 μL of the commercial enzyme solution). The final PLA2 concentration in the subphase was 482 units L^{-1} .

RESULTS AND DISCUSSION

Compression Isotherms. In order to study the influence of TEN, PIR, and MEL on the enzymatic lipolysis of phospholipid monolayers, the impact of oxicam drugs on monomolecular films formed with DLPC, DLPE, and DLPG was examined. The compression isotherms of the phospholipid monolayers spread on subphases used in the enzymatic reactions are shown in Figure 1. It can be seen that the influence of 5.0 mM CaCl_2 on the properties of the films formed with DLPC and DLPE is negligible compared to the impact of the NSAIDs and, in particular, that of MEL. This observation is not surprising, as it was shown before that Ca^{2+} does not form complexes with phosphatidylcholines.^{21,22} Only at higher concentrations of divalent cations (50 mM), a dehydration of the phosphate group due to interaction of the divalent cations with the phosphate moiety was observed using infrared reflection absorption spectroscopy.²² However, in the case of the negatively charged DLPG the effect of the increasing concentration of calcium ions is more pronounced; it can be observed even at the condensed states of the monolayers.

The characteristic parameters of the isotherms (see Experimental Section) are given in Tables 1 and 2.

Surface pressure measurements clearly show differences between the three oxicams in the monolayers. As shown in Figure 1 (solid lines), the Π – A isotherms performed in the presence of PIR or MEL in the subphase are shifted to higher molecular areas compared to pure water; the shift is more important in the case of MEL. A very small shift can be observed with TEN. In general, for MEL as well as for PIR, the shift of the isotherms decreases with the increase of surface pressure. Indeed, significant changes in phospholipid molecular areas are observed at, e.g., 15 or 30 mN m^{-1} (Table 1), while very low differences are seen at the collapse point (Table 2).

The results obtained indicate that the oxicams interact with the monolayers. The values of the compressibility modulus calculated from the Π – A isotherms (Table 1) indicate that DLPC and DLPE films spread on the subphases containing NSAIDs are more liquidlike (higher compressibility) compared to the pure phospholipid films. Moreover, the decrease of Π_{coll} values (Table 2) of monolayers in the presence of NSAIDs reflects a lower stability of the films. In general, both changes in the monolayer properties, i.e., liquefaction and destabilization of the phospholipid films induced by the drugs present in the

Table 1. Isotherm Parameters at 15 and 30 mN m⁻¹

	$\Pi = 15 \text{ mN m}^{-1}$			$\Pi = 30 \text{ mN m}^{-1}$		
	$A (\text{\AA}^2)$	$C_s^{-1} (\text{mN m}^{-1})$	$\Delta V (\text{V})$	$A (\text{\AA}^2)$	$C_s^{-1} (\text{mN m}^{-1})$	$\Delta V (\text{V})$
DLPC on pure water (0.116 μM Ca ²⁺)	67	65.9	0.37	56	103.5	0.43
DLPC on 11 μM TEN	69	66.8	0.38	57	98.5	0.44
DLPC on 11 μM PIR	72	63.1	0.39	58	88.9	0.45
DLPC on 11 μM MEL	80	47.9	0.39	63	65.5	0.45
DLPE on pure water (0.116 μM Ca ²⁺)	66	67.4	0.38	54	80.9	0.45
DLPE on 11 μM TEN	68	64.7	0.40	55	76.5	0.47
DLPE on 11 μM PIR	70	61.4	0.40	57	67.4	0.46
DLPE on 11 μM MEL	79	55.0	0.39	62	59.4	0.47
DLPG on pure water (0.116 μM Ca ²⁺)	66	49.4	0.08	51	58.9	0.13
DLPG on 11 μM TEN	69	51.4	0.24	56	85.9	0.27
DLPG on 11 μM PIR	70	51.3	0.24	56	80.9	0.29
DLPG on 11 μM MEL	73	51.0	0.25	58	79.8	0.30

Table 2. Isotherm Parameters at the Collapse Point

	Π_{coll} (mN m ⁻¹)	A_{coll} (\AA^2)	C_s^{-1} (mN m ⁻¹)	ΔV (V)
DLPC on pure water (0.116 μM Ca ²⁺)	46.5	49	121.6	0.46
DLPC on 11 μM TEN	42.0	50	114.1	0.47
DLPC on 11 μM PIR	42.1	51	100.3	0.47
DLPC on 11 μM MEL	42.7	52	81.0	0.48
DLPE on pure water (0.116 μM Ca ²⁺)	54.6	40	297.8	0.55
DLPE on 11 μM TEN	54.0	40	217.1	0.55
DLPE on 11 μM PIR	53.9	41	194.8	0.58
DLPE on 11 μM MEL	52.4	42	138.9	0.59
DLPG on pure water (0.116 μM Ca ²⁺)	40.7	41	70.5	0.16
DLPG on 11 μM TEN	44.2	47	96.3	0.32
DLPG on 11 μM PIR	43.5	47	91.2	0.33
DLPG on 11 μM MEL	43.0	49	85.4	0.34

subphase, are more significant in the case of PIR or MEL than of TEN. Interestingly, an opposite effect, that is, lower compressibility and higher stability, is observed with the negatively charged DLPG. This result indicates that the charge of the polar head plays an important role in the interaction of the phospholipids with the oxicams. We propose that the oxicams screen the negative charge and reduce the repulsive interactions between the DLPG polar heads.

As shown in Figure 1, the effect of the drugs on the surface properties of DLPC, DLPE, and DLPG monolayers can be also observed using ΔV –A measurements. Indeed, the ΔV increase characteristic for the liquid expanded–gas phase transition in DLPC and DLPE is smoothed in the presence of NSAIDs in the subphase, particularly in the case of PIR and MEL. These results indicate that there is no abrupt reorientation of molecules upon film compression; the latter is in accordance with the surface pressure isotherm results indicating liquefaction of the lipid films in the presence of the oxicams. On the other hand, the surface potential of phospholipid monolayers is higher for the films spread on the drug solution subphase compared to the films spread on pure water (Figure 1, Tables 1 and 2). The highest increase of this parameter is observed in the case of the DLPG films spread on the subphase containing MEL.

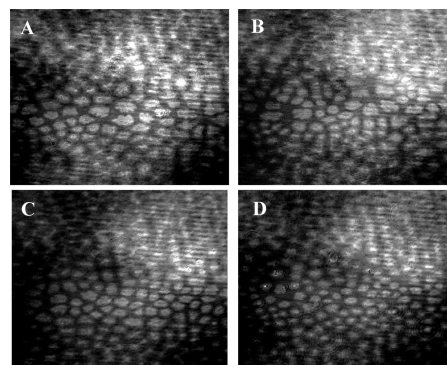


Figure 2. BAM micrographs of DLPE monolayers spread on different subphases. The snapshots were taken at 48 \AA^2 (pure water, A); 49 \AA^2 (11 μM TEN solution, B); 51 \AA^2 (11 μM PIR solution, C); 54 \AA^2 (11 μM MEL solution, D). Scale: the width of the snapshots corresponds to 254 μm .

As suggested previously, modification of the electrical properties of the lipid films by MEL could be linked to a higher lipophilicity of MEL compared to TEN and PIR.¹⁰ Due to an easier penetration to the lipid films, MEL would displace water molecules and form hydrogen bonds with the phospholipid polar heads. In general, the results obtained from the Π and ΔV measurements indicate that MEL and PIR penetrate to the monolayer from the subphase and modify the organization of the molecules and film properties to a greater extent than TEN.

Brewster Angle Microscopy. The compression isotherm measurements were completed with BAM experiments in order to visualize changes in the morphology of phospholipid monolayers upon interaction with NSAIDs. DLPE was used in those experiments because it forms characteristic, easily observed domains in the liquid expanded–liquid condensed (LE–LC) phase transition region with a plateau at a surface pressure of around 35 mN m⁻¹ (Figure 1B).

BAM images of the pure DLPE monolayers spread on pure water, as well as on the TEN, PIR, and MEL solutions, are presented in Figure 2. The snapshots were taken at the midpoint of the LE–LC phase transition for DLPE spread on pure water, as well as on the TEN, PIR, and MEL solutions.

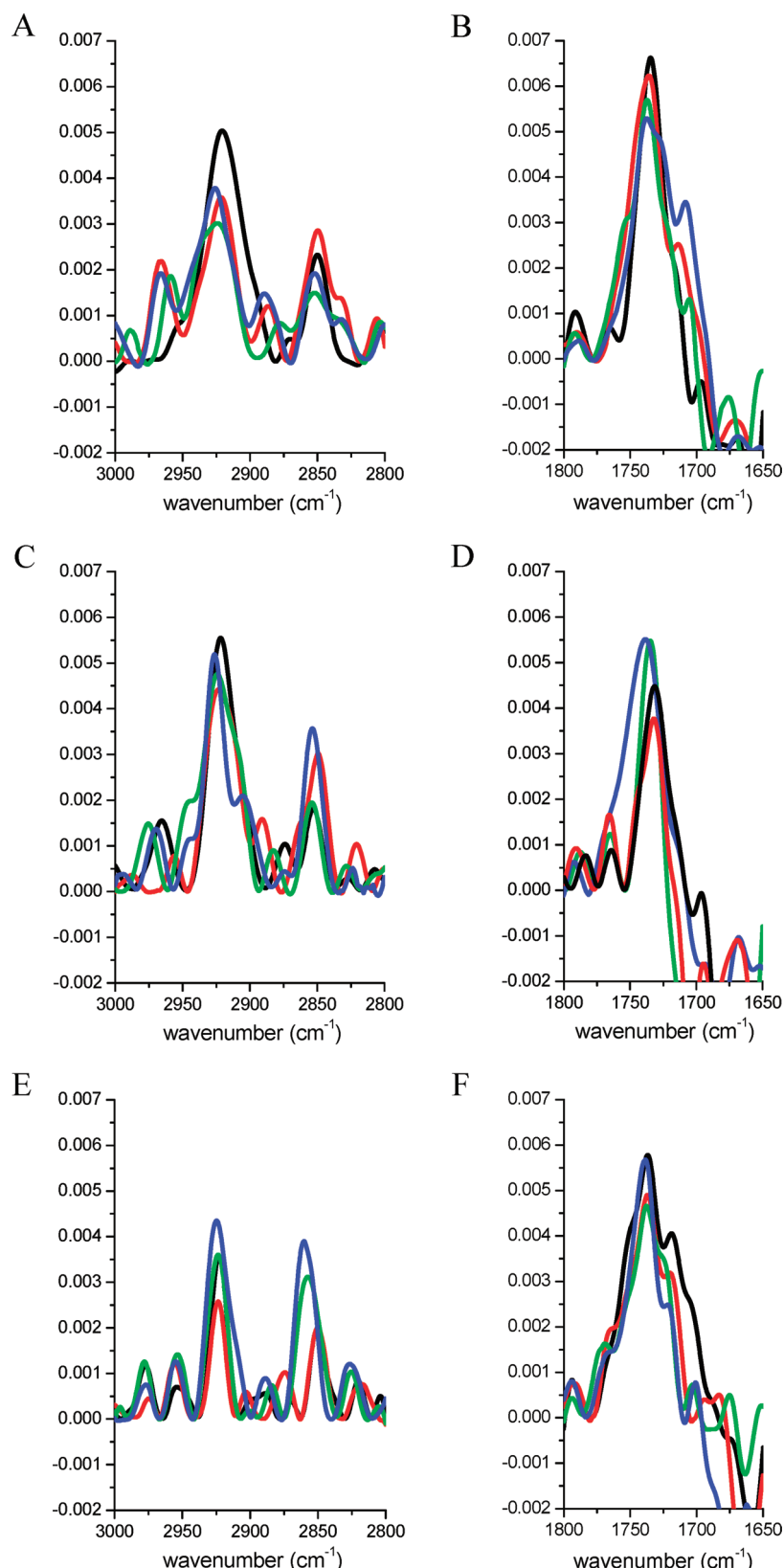


Figure 3. PM-IRRAS spectra of DLPC (A, B), DLPE (C, D), and DLPG (E, F) obtained on different subphases at 30 mN m⁻¹. Subphases: pure water (black); 11 μM TEN (red); 11 μM PIR (green); 11 μM MEL (blue). Temperature 20 °C.

The image obtained for pure DLPE monolayer formed on the pure water subphase shows numerous condensed phase domains

of irregular shapes (Figure 2A). In the presence of NSAIDs in the subphase, the size of the DLPE domains decreases and their

Table 3. Characteristic Vibrational Wavenumbers of Phospholipid Bonds upon Interaction with NSAIDs at $\Pi = 30 \text{ mN m}^{-1}$

	$\nu_{\text{as}}(\text{CH}_2)$ (cm $^{-1}$)	$\nu_s(\text{CH}_2)$ (cm $^{-1}$)	$\nu(\text{C=O})$ (cm $^{-1}$)
DLPC on pure water (0.116 $\mu\text{M Ca}^{2+}$)	2921	2851	1735
DLPC on 11 mM TEN	2922	2851	1736
DLPC on 11 $\mu\text{M PIR}$	2924	2852	1737
DLPC on 11 $\mu\text{M MEL}$	2926	2852	1738
DLPE on pure water (0.116 $\mu\text{M Ca}^{2+}$)	2922	2853	1732
DLPE on 11 $\mu\text{M TEN}$	2923	2851	1732
DLPE on 11 $\mu\text{M PIR}$	2924	2854	1735
DLPE on 11 $\mu\text{M MEL}$	2926	2854	1739
DLPG on pure water (0.116 $\mu\text{M Ca}^{2+}$)	2923	2851	1733
DLPG on 11 $\mu\text{M TEN}$	2924	2851	1737
DLPG on 11 $\mu\text{M PIR}$	2924	2857	1738
DLPG on 11 $\mu\text{M MEL}$	2925	2859	1739

number increases compared to the pure DLPE domains. This effect is least pronounced in the case of TEN (Figure 2B), followed by PIR and MEL (Figure 2C, D). The results obtained support our proposal that TEN does not penetrate into the monolayer but rather interacts with the polar heads of the phospholipids. It can be noticed that the BAM results are in agreement with the compression isotherm characteristics indicating a more liquidlike character of the films formed in the presence of MEL, followed by PIR and TEN.

PM-IRRAS Spectroscopy. PM-IRRAS studies were done to obtain more molecular-level information about changes induced by NSAIDs in the monolayers. The PM-IRRAS spectra of phospholipid films were collected on pure water or on water containing NSAIDs at 30 mN m^{-1} (Figure 3).

The influence of NSAIDs on the phospholipid monolayers was analyzed based on the frequency of the lipid symmetric and antisymmetric methylene group stretching vibrations, $\nu_s(\text{CH}_2)$ and $\nu_{\text{as}}(\text{CH}_2)$, respectively, and the ester carbonyl stretching band $\nu(\text{C=O})$.^{23–26}

CH_2 Stretching Region. The CH_2 stretching region is located between 2800 and 3000 cm $^{-1}$; the two dominating peaks are observed in the phospholipid spectra around 2920 and 2850 cm $^{-1}$, which correspond to the antisymmetric and symmetric methylene group stretching vibrations, respectively. The frequencies of these bands are sensitive to the conformation of phospholipid acyl chains^{27–29} and thus provide valuable information on the orientation of lipid acyl chains in the membrane. Indeed, downward shift of the $\nu_{\text{as}}(\text{CH}_2)$ and $\nu_s(\text{CH}_2)$ frequencies from 2920 and 2850 cm $^{-1}$ indicates higher chain ordering in the film, i.e., an ordered all-trans conformation of the chains, while their upward shift suggests chain disordering with increase in the number of gauche conformers in the chain.²⁸

The characteristic vibrations of phospholipids, namely the antisymmetric and symmetric methylene stretching vibrations, are clearly visible in the spectra of pure phospholipids (Figure 3A, C, black curves). In the pure lipid monolayers, the $\nu_{\text{as}}(\text{CH}_2)$ and $\nu_s(\text{CH}_2)$ bands appear at wavenumbers slightly higher than 2920 and 2850 cm $^{-1}$, respectively (Table 3). Those peak positions are

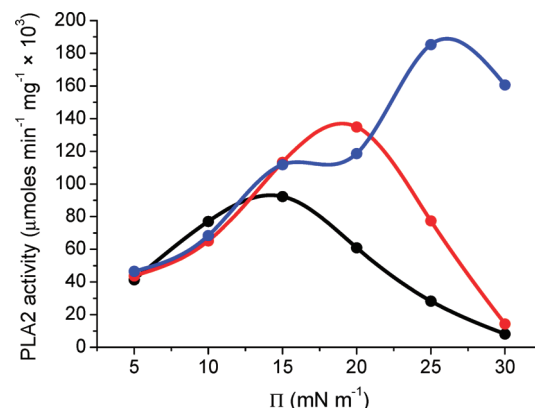


Figure 4. PLA2 activity on DLPC (black), DLPE (red), and DLPG (blue) monolayers spread on Milli-Q water containing 5 mM CaCl_2 as a function of surface pressure.

typical for liquid expanded films with disordered acyl chains, which is in agreement with the compression isotherm analysis (Table 1).

In the case of monolayers formed in the presence of NSAIDs, the compression isotherm analysis clearly shows that MEL and PIR penetrate to the monolayers from the subphase and change the monolayer ordering (Figure 1, Table 1). The conformational changes of phospholipid chains show in the $\nu_{\text{as}}(\text{CH}_2)$ and $\nu_s(\text{CH}_2)$ band wavenumbers, which are shifted to higher values compared to the pure DLPC and DLPE monolayers (Figure 3, Table 3). This effect suggests that penetration of MEL and PIR to the monolayer favors phospholipid chain disordering; i.e., the number of gauche conformers in the chains increases.

Compared to the monolayers spread on MEL and PIR solution, TEN does not cause any significant shift of the CH_2 band frequencies. This result indicates that phospholipid chain orientation remains unchanged in the presence of TEN.

Carbonyl Stretching Region. The $\nu(\text{C=O})$ stretching band observed at around 1730 cm $^{-1}$ is often used to investigate the interfacial region of phospholipids. However, the ester carbonyl C=O stretching band is quite complex because it appears to be the summation of two overlapping bands.^{30,31} The frequency of this band depends on the hydration of the ester group and thus provides useful information concerning changes in the hydration. Indeed, in a given phospholipid, the low- and high-frequency bands correspond, respectively, to hydrated and dry carbonyl groups.³²

The PM-IRRAS spectra of pure DLPC, DLPE, and DLPG monolayers display stretching $\nu(\text{C=O})$ bands at around 1735, 1732, and 1733 cm $^{-1}$, respectively. While no significant influence of TEN on the $\nu(\text{C=O})$ band can be observed (Table 3), a clearly visible shift of this band to higher wavenumbers occurs in the case of PIR and MEL. This effect indicates dehydration of carbonyl moieties and a decrease of the number of hydrogen-bonded carbonyl groups.

All PM-IRRAS results taken together are in accordance with those obtained from the compression experiments and indicate interaction between NSAIDs and phospholipid molecules. However, the less polar PIR and MEL penetrate more easily to the lipid films and induce changes in the orientation of the hydrocarbon chains compared to the more polar TEN present in the water subphase in the polar head region. MEL induces the most significant changes both in the hydrocarbon chain organization

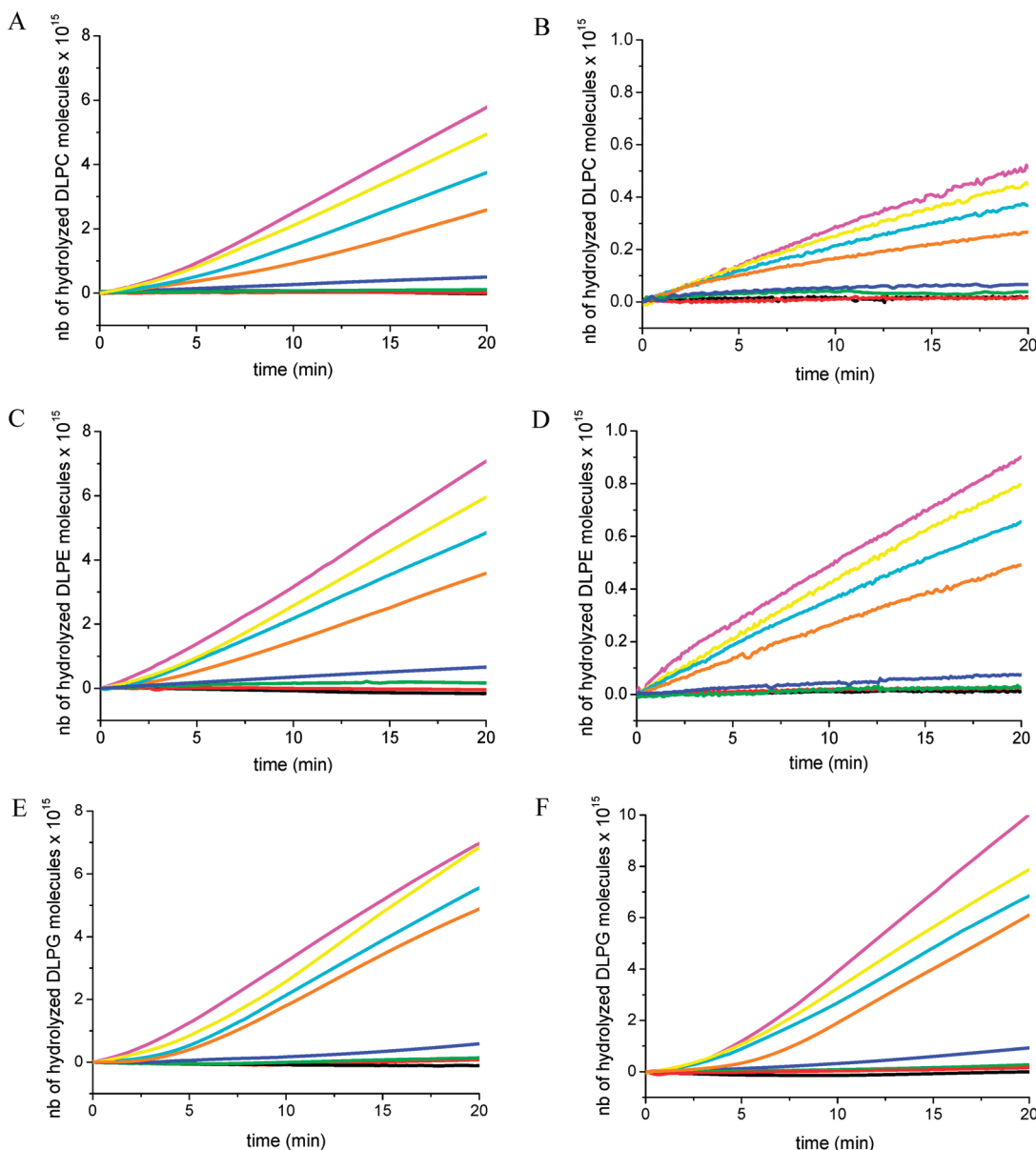


Figure 5. Kinetics of hydrolysis of DLPC (A, B), DLPE (C, D), and DLPG (E, F) monolayers spread on different subphases, catalyzed by PLA2 at 15 (A, C, E) and 30 mN m⁻¹ (B, D, F). Subphases: pure water (black); 5.0 mM CaCl₂ (magenta); 11 μM TEN (red); 5.0 mM CaCl₂ + 11 μM TEN (yellow); 11 μM PIR (green); 5.0 mM CaCl₂ + 11 μM PIR (cyan); 11 μM MEL (blue); 5.0 mM CaCl₂ + 11 μM MEL (orange). The concentration of Ca²⁺ cations measured with ICP-MS was 25.27 ng mL⁻¹ (0.631 μM) in TEN solutions, 9.84 ng mL⁻¹ (0.246 μM) in PIR solutions, 7.80 ng mL⁻¹ (0.195 μM) in MEL solutions, and 4.67 ng mL⁻¹ (0.116 μM) in pure Milli-Q water. Temperature 20 °C.

and in the carbonyl dehydration; it should be noted that MEL is the most hydrophobic among the oxicams studied.¹⁰

Enzymatic Lipolysis. The eukaryotic PLA2 plays a pivotal role in the inflammatory process. Indeed, it selectively catalyzes hydrolysis of the *sn*-2 ester bond in phosphoglycerides yielding a lysophospholipid and a fatty acid, which is the precursor in the biosynthesis of prostaglandins and other mediators of inflammation.

Here, PLA2 enzyme was used as a probe differentiating between the phospholipid monolayers in the presence and in the absence of NSAIDs. In order to generate water-soluble products necessary for monitoring enzyme activity, medium-length-chain DLPC, DLPE, and DLPG were used as substrates.^{11,16} Moreover, because of the calcium dependence of PLA2, enzymatic reactions were performed in the presence of

Ca²⁺ in the subphase. In order to check the influence of Ca²⁺ on the properties of the phospholipid monolayers, the Π-A isotherms of pure lipids spread on subphases used in the enzymatic reactions were measured. As demonstrated previously, the presence of 5 mM CaCl₂ in the subphase does not influence the Π-A profiles of the phospholipid isotherms.¹⁶

The enzymatic lipolyses of the monolayers spread on the 5 mM CaCl₂ solution were performed at different surface pressures (results not shown).

As expected on the basis of the literature, the reaction rate depends on the state of the monolayer.¹⁷ The PLA2 activity calculated from the kinetic data shows maxima at around 15, 20, and 25 mN m⁻¹ in the cases of DLPC, DLPE, and DLPG, respectively (Figure 4).

Table 4. PLA2 Activity in the Presence and Absence of NSAIDs in the Subphase

subphase composition	$\Pi = 15 \text{ mN m}^{-1}$		$\Pi = 30 \text{ mN m}^{-1}$	
	reaction rate [$\mu\text{mol min}^{-1} \times 10^3$]	PLA2 activity [$\mu\text{mol min}^{-1} \text{ mg}^{-1} \times 10^3$]	reaction rate [$\mu\text{mol min}^{-1} \times 10^3$]	PLA2 activity [$\mu\text{mol min}^{-1} \text{ mg}^{-1} \times 10^3$]
DLPC				
5.0 mM CaCl ₂	0.480	92.29	0.043	8.22
5.0 mM CaCl ₂ + 11 μM TEN	0.413	79.44	0.037	7.08
5.0 mM CaCl ₂ + 11 μM PIR	0.312	60.08	0.031	5.90
5.0 mM CaCl ₂ + 11 μM MEL	0.216	41.56	0.022	4.23
pure water (0.116 μM Ca ²⁺)	0	0	0	0
11 μM TEN	0.002	0.38	0.001	0.21
11 μM PIR	0.012	2.40	0.003	0.49
11 μM MEL	0.042	8.11	0.005	0.85
DLPE				
5.0 mM CaCl ₂	0.589	113.27	0.075	14.39
5.0 mM CaCl ₂ + 11 μM TEN	0.511	98.35	0.066	12.75
5.0 mM CaCl ₂ + 11 μM PIR	0.404	77.67	0.055	10.51
5.0 mM CaCl ₂ + 11 μM MEL	0.298	57.32	0.041	7.86
pure water (0.116 μM Ca ²⁺)	0	0	0	0
11 μM TEN	0.005	0.88	0.001	0.21
11 μM PIR	0.015	2.93	0.004	0.77
11 μM MEL	0.061	11.73	0.006	1.14
DLPG				
5.0 mM CaCl ₂	0.582	111.84	0.836	160.72
5.0 mM CaCl ₂ + 11 μM TEN	0.571	109.76	0.658	126.59
5.0 mM CaCl ₂ + 11 μM PIR	0.464	89.15	0.572	110.01
5.0 mM CaCl ₂ + 11 μM MEL	0.408	78.41	0.510	98.06
pure water (0.116 μM Ca ²⁺)	0	0	0	0
11 μM TEN	0.007	1.26	0.013	2.52
11 μM PIR	0.012	2.29	0.023	4.36
11 μM MEL	0.049	9.48	0.078	14.98

Basing on the results above, the enzymatic lipolysis of the monolayers spread on subphases containing NSAIDs was performed at a surface pressure of 15 mN m^{-1} ; 30 mN m^{-1} was used because it is relevant for biological membranes.³³

The reaction kinetics are shown in Figure 5. Contrary to the subphase containing 5 mM CaCl₂ (Figure 5, magenta curves), in the case of films spread on pure Milli-Q water no catalytic activity was detected (Figure 5, black curves).¹⁶ However, it is important to mention that Milli-Q water contained trace amounts of Ca²⁺ (0.116 μM), as determined with ICP-MS.

In the case of subphases containing 5 mM CaCl₂ and one of the three NSAIDs, the decrease of the reaction rate was observed compared to the subphase containing only 5 mM CaCl₂ (Figure 5, Table 4). This effect was observed at both 15 and 30 mN m^{-1} ; it was more important in the cases of MEL and PIR than in the case of TEN. Indeed, for DLPC, DLPE, and DLPG monolayers and MEL/5 mM CaCl₂ in the subphase (Figure 5, orange curves) the reaction rates were, respectively, around 2.2, 2.0, and 1.4 times lower compared to that for the 5 mM CaCl₂ subphase (Figure 5, magenta curves). The smallest changes in the reaction rate were observed in the case of TEN and 5 mM CaCl₂ in subphase; namely the decrease was around 1.2, 1.1, and 1.0 times for DLPC, DLPE, and DLPG monolayers, respectively. PIR yielded an intermediary effect.

On the other hand, in the presence of trace amounts of Ca²⁺ (0.116 μM Ca²⁺) in the pure water subphase, an increase of the rate of hydrolysis of both lipids was clearly visible in the presence of MEL (Figure 5, blue curves, and Table 4) in contrast to the pure water subphase (Figure 5, black curves, and Table 4). Also some enhancement of the reaction rate was observed in the presence of PIR (Figure 5, green curves, and Table 4) compared to the PIR-free subphase (Figure 5, black curves, and Table 4). In the case of TEN a very low enhancement of the reaction rate was observed (Figure 5, red curves) compared to pure water (Figure 5, black curves, and Table 4). The increase of the reaction rate observed in the presence of NSAIDs in the subphase could be associated with penetration of the drugs to the lipid film and modification of the film properties. Indeed, MEL and PIR have a more significant impact on the monolayer properties than TEN.

The enzymatic reaction rate for the surface pressure of 30 mN m^{-1} in the presence of NSAIDs and trace amounts of Ca²⁺ exhibits the same tendency as in the case of enzymatic reaction preformed at 15 mN m^{-1} (Figure 5, Table 4). Namely, MEL has the most important impact on both the decrease and increase of the reaction rate, followed by PIR and TEN. Interestingly, at 30 mN m^{-1} the enhancement of the reaction rate is around 1 order of magnitude higher with DLPG compared to

DLPC and DLPE. As suggested by the compression isotherms (Figure 1), the interaction with the oxicams may be stronger in the case of the negatively charged polar heads compared to the zwitterions; the resulting screening of the charge may facilitate the interaction of PLA2 with the substrate upon adsorption to the film, which is the first step of the catalysis.

CONCLUSIONS

The enzymatic experiments showed that TEN, PIR, or MEL modulates, that is, decreases or increases the reaction rate of PLA2-catalyzed lipolysis depending on the concentration of calcium ions. Interestingly, this effect is the most important in the case of MEL and the least important in the case of TEN. We propose that the NSAIDs studied act as PLA2 effectors.³⁴ Indeed, allosteric interactions can inhibit or activate enzymes, and are a common way that enzymes are controlled in the body.³⁵

On the other hand, it can be observed that the impact of the three NSAIDs on the catalysis rate correlates with the modification of the physicochemical properties of the film: among the three oxicams studied, MEL has the most significant impact both on the film properties and on the reaction rate. This effect indicates that PLA2 recognizes different physicochemical states of the film induced by third molecules. The role of the charge is shown to be essential in this process as demonstrated with the negatively charged DLPG.

While a detailed molecular mechanism of the phenomena observed is elusive at the moment, these observations may be important both for a better understanding of the mechanism of the PLA2-lipid interaction and for pharmacological applications.

AUTHOR INFORMATION

Corresponding Author

*E-mail: rogalska@uhp-nancy.fr. Telephone: +33 (0)3 83 68 43 45. Fax: +33 (0)3 83 68 43 22.

ACKNOWLEDGMENT

This work was supported by the Ministry of Science and Higher Education, Poland, and EGIDE, France, within the framework of the French-Polish collaboration “Polonium” and GDRE (Project No. 1206/GDR/2007/03). We thank Halina Mrowiec for trace analysis. The technical assistance of Francis Hoffmann is gratefully acknowledged.

REFERENCES

- (1) Kulkarni, S. K.; Jain, N. K.; Singh, A. *Methods Find. Exp. Clin. Pharmacol.* **2000**, *22*, 291–298.
- (2) Picot, D.; Loll, P. J.; Garavito, R. M. *Nature* **1994**, *367*, 243–249.
- (3) Spencer, A. G.; Woods, J. W.; Arakawa, T.; Singer, I. I.; Smith, W. L. *J. Biol. Chem.* **1998**, *273*, 9886–9893.
- (4) Luger, P.; Danneck, K.; Engel, W.; Trummlitz, G.; Wagner, K. *Eur. J. Pharm. Sci.* **1996**, *4*, 175–187.
- (5) Scott, K. F.; Bryant, K. J.; Bidgood, M. J. *J. Leukocyte Biol.* **1999**, *66*, 535–541.
- (6) Wu, K. K.; Liou, J.-Y. *Biochem. Biophys. Res. Commun.* **2005**, *338*, 45–52.
- (7) Peters, A. R.; Dekker, N.; van den Berg, L.; Boelens, R.; Kaptein, R.; Slotboom, A. J.; de Haas, G. H. *Biochemistry* **1992**, *31*, 10024–10030.
- (8) Ferreira, H.; Lucio, M.; Lima, J. L. F. C.; Cordeiro-da-Silva, A.; Tavares, J.; Reis, S. *Anal. Biochem.* **2005**, *339*, 144–149.
- (9) Ruan, K.-H.; Deng, H.; Wu, J.; So, S.-P. *Arch. Biochem. Biophys.* **2005**, *435*, 372–381.
- (10) Czapla, K.; Korczowiec, B.; Rogalska, E. *Langmuir* **2010**, *26*, 3485–3492.
- (11) Corvis, Y.; Barzyk, W.; Brezesinski, G.; Mrabet, N.; Badis, M.; Hecht, S.; Rogalska, E. *Langmuir* **2006**, *22*, 7701–7711.
- (12) Korczowiec, B.; Ben Salem, A.; Corvis, Y.; Regnouf-de-Vains, J.-B.; Korczowiec, J.; Rogalska, E. *J. Phys. Chem. B* **2007**, *111*, 13231–13242.
- (13) Kivinen, A.; Vikholm, I.; Tarpila, S. *Int. J. Pharm.* **1994**, *108*, 109–115.
- (14) Lygre, H.; Moe, G.; Holmsen, H. *Acta Odontol. Scand.* **2003**, *61*, 303–309.
- (15) Souza, S. M. B.; Oliveira, O. N.; Scarpa, M. V.; Oliveira, A. G. *Colloids Surf., B* **2004**, *36*, 13–17.
- (16) Wieclaw, K.; Korczowiec, B.; Corvis, Y.; Korczowiec, J.; Guermouche, H.; Rogalska, E. *Langmuir* **2009**, *25*, 1417–1426.
- (17) Verger, R.; De Haas, G. H. *Chem. Phys. Lipids* **1973**, *10*, 127–136.
- (18) Tsai, R. S.; Carrupt, P. A.; El Tayar, N.; Giroud, Y.; Andrade, P.; Testa, B.; Bree, F.; Tillement, J. P. *Helv. Chim. Acta* **1993**, *76*, 842–854.
- (19) Naidu, N. B.; Chowdary, K. P. R.; Murthy, K. V. R.; Satyanarayana, V.; Hayman, A. R.; Becket, G. *J. Pharm. Biomed. Anal.* **2004**, *35*, 75–86.
- (20) David, V.; Albu, F.; Medvedovici, A. *J. Liq. Chromatogr. Relat. Technol.* **2004**, *27*, 965–984.
- (21) Corvis, Y.; Korczowiec, B.; Brezesinski, G.; Foliot, S.; Rogalska, E. *Langmuir* **2007**, *23*, 3338–3348.
- (22) Gromelski, S.; Brezesinski, G. *Langmuir* **2006**, *22*, 6293–6301.
- (23) Blaudez, D.; Buffeteau, T.; Cornut, J. C.; Desbat, B.; Escafre, N.; Pezolet, M.; Turlet, J. M. *Appl. Spectrosc.* **1993**, *47*, 869–874.
- (24) Blaudez, D.; Buffeteau, T.; Cornut, J. C.; Desbat, B.; Escafre, N.; Pezolet, M.; Turlet, J. M. *Thin Solid Films* **1994**, *242*, 146–150.
- (25) Blaudez, D.; Turlet, J.-M.; Dufourcq, J.; Bard, D.; Buffeteau, T.; Desbat, B. *J. Chem. Soc., Faraday Trans.* **1996**, *92*, 525–530.
- (26) Cornut, I.; Desbat, B.; Turlet, J. M.; Dufourcq, J. *Biophys. J.* **1996**, *70*, 305–312.
- (27) Snyder, R. G.; Strauss, H. L.; Elliger, C. A. *J. Phys. Chem.* **1982**, *86*, 5145–5150.
- (28) Meister, A.; Kerth, A.; Blume, A. *J. Phys. Chem. B* **2004**, *108*, 8371–8378.
- (29) Dicko, A.; Bourque, H.; Pezolet, M. *Chem. Phys. Lipids* **1998**, *96*, 125–139.
- (30) Lewis, R. N.; McElhaney, R. N.; Pohle, W.; Mantsch, H. H. *Biophys. J.* **1994**, *67*, 2367–2375.
- (31) Blume, A.; Huebner, W.; Messner, G. *Biochemistry* **1988**, *27*, 8239–8249.
- (32) Allouche, M.; Castano, S.; Colin, D.; Desbat, B.; Kerfelec, B. *Biochemistry* **2007**, *46*, 15188–15197.
- (33) Yokoyama, S.; Ohta, Y.; Sakai, H.; Abe, M. *Colloids Surf., B* **2004**, *34*, 65–68.
- (34) Kamata, K.; Mitsuya, M.; Nishimura, T.; Eiki, J.-i.; Nagata, Y. *Structure (Cambridge, MA, U. S.)* **2004**, *12*, 429–438.
- (35) Changeux, J.-P.; Edelstein, S. J. *Science (Washington, DC, U. S.)* **2005**, *308*, 1424–1428.